Location of Spectroscopic Probes in Self-Aggregating Assemblies. I. The Case for 5-Doxylstearic Acid Methyl Ester Serving as a Benchmark Spectroscopic Probe to Study Micelles

Nataly Lebedeva[†,‡] and Barney L. Bales*[,†]

Department of Physics and Astronomy and the Center for Supramolecular Studies, California State University at Northridge, Northridge, California 91330-8268, and International Tomography Center, SB RAS, Institutskaya st. 3a, Novosibirsk 630090, Russia

Received: January 24, 2006; In Final Form: March 8, 2006

A strategy to locate spectroscopic probes in micelles is presented which involves establishing a "benchmark" probe, i.e., one whose position is well-known and against which other probe positions may be established. Theoretically calculated values of the fraction of the micelle polar shell occupied by water, H_{shell}, are compared with experimental values measured with the spin probe 5-doxylstearic acid methyl ester (5DSE) for a series of sodium *n*-alkyl sulfate micelles as functions of both the aggregation numbers and the alkyl chain length. The theoretical values involve one adjustable parameter that may be taken to be the volume in the polar shell inaccessible to water, V_{dry}. Under the hypothesis that the thickness of the polar shell (5 Å) remains constant as either the aggregation number or the chain length is varied, we find excellent agreement between the theoretical predictions and the experimental results, using the same value of V_{dry} for chain lengths 8−12 and for aggregation numbers varying from approximately 38 to 130. We argue that these are compelling reasons that 5DSE follows the zero-order model (ZOM) of probe location. The ZOM applies to any probe that rapidly diffuses within the confines of the micelle polar shell and nowhere else. Thus, 5DSE can serve as a benchmark in the sodium alkyl sulfate micelles. As a further check, results are also presented for ammonium dodecyl sulfate micelles, where 5DSE is also found to follow the ZOM, i.e, no further adjustable parameters are needed to pass from the sodium alkyl sulfate micelles to ammonium dodecyl sulfate micelles. In contrast, results are also presented for a similar spin probe 16-doxylstearic acid methyl ester (16DSE) that is found *not* to adhere to the ZOM in any of the micelles. A simple first-order correction to the ZOM in which 16DSE is displaced slightly from the polar shell is shown to account for the results well. The necessary displacements, which range from about 0.7 Å outside the polar shell to 1.3 Å inside, are not correlated with either chain lengths or aggregation numbers; however, they correlate rather well with H_{shell}. Calibrations of 6-, 7-, 10-, and 12DSE spin probes are presented in the Appendix, making them available to measure microviscosities and effective water concentrations.

Introduction

One of the chief uses, by nature and man, of self-assembled aggregates such as micelles is to transport molecules that are sparingly water-soluble into the aqueous phase. A deep understanding of the behavior of these hydrophobic molecules in chemistry and biology requires detailed knowledge of at least the following two items: (1) the structure and the physicochemical properties of the aggregate and (2) the location of the solubilized guest molecule. The case for the need for item (1) was nicely detailed in Grieser and Drummond's review.[1] The need for item (2) seems self-evident, and a number of workers have attempted to shed light on the problem by employing spectroscopic probes. For example, already in 1979, Almgren et al.[2] showed that aromatic fluorescent probes and aromatic or ionic quenchers reside preferentially in the polar shell. A few years later, Kevan and co-workers[3,4] applied electron spin−echo modulation (ESEM) to nitroxide spin probes in micelles. Those workers concluded that some of these probes were located near the micelle surface. One concern with the work was the fact that the micelle solution was frozen, so one had to assume that the structure was maintained. More recently, Szajdzinska-Pietek and co-workers have continued the quest to locate nitroxide spin probes in micelles, exploiting their ability to quench pyrene[5] fluorescence and to scavenge radiolytically produced electrons.[6]

Micelles are dynamic structures, thus guest molecules cannot be located in the usual sense of defining the position of their atoms relative to a coordinate system in the host; thus, we take the word "locate" to mean to define the *average* position relative to the structural properties of the aggregate. One uses a wide variety of techniques to reach a consistent model of the structure. In our opinion, only then do probes become useful. Probes may then be used to refine the structural model. Finally, if systematic variation of the structure can be effected, the location of the probe in favorable conditions may be deduced.

In recent papers, [7−10] we advanced a tentative proposal that the nitroxide moiety (NO•) of 5-doxylstearic acid methyl ester (5DSE) diffuses exclusively throughout the Stern layer of sodium dodecyl sulfate micelles. We call this location of a spectroscopic probe the zero-order model (ZOM). That proposal was based upon the comparison of a theoretically predicted volume fraction of water in the Stern layer, H_{shell}, with that

* Corresponding author. E-mail: barney.bales@csun.edu. Webpage: http://www.csun.edu/~vcphy00s/BBVita.html.

† Department of Physics and Astronomy and the Center for Supramolecular Studies, California State University at Northridge.

‡ International Tomography Center, SB RAS.

10.1021/jp060515y CCC: $33.50
Published on Web 04/28/2006

TABLE 1: Parameters for *n*-Alkyl Sulfate and Ammonium Dodecyl Sulfate Micelles

	t, °C	cmc_0, mM	N^0	γ	α	V_{hg}, Å^3 ($N_{wet} = 0$)	$(1-\alpha)V_{ci}$, Å^3	N_{wet} ($V_{hg} = 66.4$ Å^3)
S8S	25	134[20]	38[18]	0.25[18]	0.42[18]	126	0	1.70
S9S	25	64.5[20]	35[18]	0.25[18]	0.41[18]	129	0	1.83
S10S	25	30[20]	45[18]	0.20[18]	0.35[18]	130	0	1.86
S11S	25	14.1[20]	52[18]	0.18[18]	0.30[18]	130	0	1.91
S12S	25	8.3[49]	50[50]	0.25[22]	0.27[17]	129	0	1.91
Am12S	16	7.2[13]	61[13]	0.22[13]	0.22[13]	127	15	1.88
Am12S	25	7.1[13]	70[13]	0.22[13]	0.23[13]	128	15	1.91
Am12S	35	7.3[13]	77[13]	0.22[13]	0.25[13]	129	15	2.20

measured by the spin probe as a function of the aggregation number, N. One parameter is adjustable in the theory, so theory and experiment can always be made to coincide for any given value of N; nevertheless, in all work to date,[7,9,11−13] that one adjusted parameter was reasonable, in conformity with expectations and other experimental methods.[14,15] Moreover, the variation of H_{shell} with N is not adjustable, so the ZOM drew its greatest strength from the fact that this variation was the same experimentally and theoretically.[7−10] In earlier work, we suggested[7] that varying the chain length of the normal sodium *n*-alkysulfate surfactants (SN_cS, where N_c is number of carbons in the alkyl chain) would be a further severe test of the ZOM. The reason is that, in addition to varying N, one may vary the relative size of the surfactant to the probe from 44 to 77% in terms of number of carbons. The ZOM should predict, a priori, the results of the experiments for all values of N_c under the reasonable hypothesis that the Stern layer of the micelles is the same thickness. No further adjustable parameters are admitted. Even if there are uncertainties in the values of some of the parameters in the theory, the relative values as functions of N and N_c ought to be reliable. The purpose of this paper is to show that 5DSE is described by the ZOM for SN_cS, $N_c = 8-12$ as well as for ammonium dodecyl sulfate (Am12S) micelles. The short companion paper[16] immediately following this paper shows that 5DSE is also described by the ZOM in cationic dodecyl trimethylammonium bromide (DTAB) micelles.

Therefore, 5DSE is an excellent candidate to provide a gateway into the location of other spectroscopic probes. We borrow the term "benchmark" from the field of surveying to denote a molecule whose location is known and may thus serve as a basis to locate others through its interactions with them. A benchmark need not follow the ZOM as long as we know where it resides in a given micelle as experimental parameters are varied. A nitroxide spin probe is particularly suited to be a benchmark because the location of NO•, effectively confined to the dimensions of the unpaired spin−orbital, is well defined, unlike other spectroscopic probes, e.g., pyrene.

A second purpose of the work is to provide a negation of the hypothesis that 5DSE follows the ZOM. This is accomplished by employing 16-doxylstearic acid methyl ester (16DSE) in all of the micelles consider here and in DTAB in the companion paper. We show that it is very easy to detect variations from the ZOM; departures of NO• from the polar shell as small as 0.2 Å may be measured.

A program establishing the location of a wide variety of spectroscopic probes is tedious. In the beginning, the detailed location of the benchmark is subject to uncertainties. As more probes are studied, the constraint imposed by their mutual interactions will serve to refine earlier assignments, reducing the uncertainties. Early in the process, location assignments must be tentative and will most likely need to be refined as more probes are employed.

Theory

Variation of N. A critical tool in our investigation is the ability to vary N systematically. It is fortunate indeed that one may vary N in ionic micelles systematically by varying either the surfactant or the added-salt concentrations.[17,18] There are at least two reasons for this. First, one may check for intermicellar interactions by comparing micelles with the same value of N but different micelle concentrations. Second, measurements at the cmc, for example, from light scattering,[19,20] may be placed on the same footing[21] as those well above the cmc. For many micelles, including all of those investigated in this paper, N varies as follows:

$$N = N^0(C_{aq}/\mathrm{cmc}_0)^{\gamma} \tag{1}$$

where N^0 is the aggregation number at the cmc in the absence of added salt, cmc_0, γ is a constant, and C_{aq} is the concentration of counterions in the aqueous phase given by

$$C_{aq} = [\alpha C + (1-\alpha)C_{free} + C_{ad}]/(1 - VC) \tag{2}$$

C and C_{free} are the concentrations of total surfactant and of monomer surfactant, respectively, and C_{ad} is the concentration of added common counterion in the form of salt. All concentrations are in mol/L. V is the molar volume of the anhydrous surfactant, and α is the degree of micelle ionization. C_{free} is computed from eq 5 of ref 22. The reader is referred to recent papers where we have thoroughly discussed the computation of C_{aq} and the variation of N.[17,21,23−25] Parameters in eqs 1 and 2 are given in Table 1.

Model of Micelle Hydration. We employ the same model used in recent papers[7−9,11,12,21,25] based upon a classical picture of a nearly spherical micelle having a hydrocarbon core with very little water penetration, surrounded by a polar shell. Figure 1 shows a schematic of the model and defines the core and micelle radii, R_c and R_m, respectively. For a beautiful 3D schematic of an S12S micelle generated from molecular dynamics calculations by A. D. MacKerell, Jr.,[26] see ref 27.

The polar shell contains N headgroups (hg), $N(1-\alpha)$ counterions (ci), an average number of methylene groups per surfactant molecule, N_{wet}, and water. At a given temperature, the thickness of the polar shell is taken to be constant as functions of either N or N_c. A simple continuum model is used in which the volumes occupied by the headgroups, V_{hg}, the counterions, V_{ci}, and the methylene groups, V_{CH_2} is inaccessible to water (dry), and the rest of the polar shell is filled with water. The volume fraction of the polar shell occupied by water, H_{shell}, is therefore given by

$$H_{shell} = \frac{V_{shell} - V_{dry}}{V_{shell}} \tag{3}$$

where

$$V_{\text{shell}} = \frac{4\pi}{3}(R_m^{\ 3} - R_c^{\ 3}) \tag{4}$$

and

$$V_{\text{dry}} = N[V_{\text{hg}} + (1-\alpha)V_{\text{ci}} + N_{\text{wet}}V_{\text{CH}_2}] \tag{5}$$

The core radius is found from

$$NV_{\text{tail}} = \frac{4\pi}{3}R_c^{\ 3} \tag{6}$$

where V_{tail} is the volume of the hydrocarbon chain embedded in the core, computed according to Tanford[28] as follows:

$$V_{\text{tail}} = 27.4 + 26.9(N_c - N_{\text{wet}}) \tag{7}$$

Equations 3−7 yield the value of H_{shell} for any micelle, anionic, cationic, or nonionic (leaving out ci) that can reasonably be modeled as Figure 1.

At a given value of N, the value of H_{shell} in eq 3 depends on the shell thickness, the values of the molar volumes of the constituents, and N_{wet}. In principle, all of these parameters could be determined by independent experiments; however, in practice, all have uncertainties. In our past work, we have fixed the shell thickness to be the diameter of the larger of the headgroup or the counterion and adjusted one parameter. For SN_cS, $R_m - R_c = 5$ Å. A natural fitting parameter is V_{dry} in eq 3, fixing the parameters that define V_{shell}. Various combinations of V_{hg} and N_{wet} give the same value of V_{dry}. Of these, we present two in Table 1 by giving values of N_{wet} fixing[29] $V_{\text{hg}} = 66.4$ Å^3 or values of V_{hg} fixing $N_{\text{wet}} = 0$. The number of water molecules per surfactant molecule or the effective water concentration may easily be computed from the value of V_{dry}.[7]

Spin-Probe Sensed Values of *H*. From the EPR of these spin probes, the hyperfine spacing between the low- and center-field resonances, A_+, may be measured with excellent precision.[17] Theoretically, A_+ is well understood; see, for example, refs 30−38. Mukerjee et al.[31] introduced a nonempirical polarity scale, H, defined to be the ratio of molar concentration of OH dipoles in a solvent or solvent mixture to that in water that shows

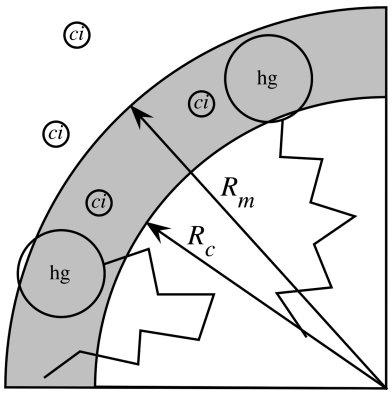

Figure 1. Schematic representation of the core−shell model of a spherical micelle showing the micelle radius, R_m, the core radius, R_c, the headgroups, hg, and the counterions, ci. The volume fraction of the shell occupied by water, H_{shell}, is found by subtracting the volumes occupied by ci, hg, and any portion of the alkyl chains that reside within the shell from the volume of the shell and dividing by the volume of the shell.

TABLE 2: Parameters of Eq 8 and Hydrodynamic Radii of *x*DSE, 25 °C

	$A+(0)$, G	$\partial A_+/\partial H$, G	R_h, Å
5DSE	14.301 ± 0.010[13]	1.380 ± 0.016[13]	4.7 ± 0.1 Å[42]
6 DSE	14.312 ± 0.013	1.387 ± 0.023	4.7 ± 0.1 Å
7 DSE	14.301 ± 0.012	1.427 ± 0.021	4.8 ± 0.1 Å
10 DSE	14.304 ± 0.007	1.446 ± 0.012	5.1 ± 0.1 Å
12 DSE	14.313 ± 0.007	1.441 ± 0.011	4.6 ± 0.1 Å
16 DSE	14.309 ± 0.009[11]	1.418 ± 0.013[d]	3.75 ± 0.08 Å[12]

excellent linear correlation with values of A_+

$$A_+ = A_+^{\ 0} + \frac{\partial A_+}{\partial H}H_{\text{NO}\bullet} \tag{8}$$

with constant $(\partial A_+/\partial H)$. Equation 8 has been calibrated for 5DSE[13] and 16DSE[11] in solvents and mixtures in the literature. In this work, we have measured other *x*DSE probes, where $x =$ 6, 7, 10, and 12 is the attachment point of the doxyl group. Values of the constants $A_+^{\ 0}$ and $(\partial A_+/\partial H)$ are found as detailed in the Appendix and are given in Table 2.

Provided that the solvent mixture of interest is water and molecules possess no OH bonds or other hydrogen-bonding molecules, $H_{\text{NO}\bullet}$ is the volume fraction occupied by water.

In this paper, we use the phrase "locate *x*DSE" to mean that we define the average location of its nitroxide moiety, NO•, by means of interactions with the micelle. With this meaning, we shall show that 5DSE and 16DSE are similarly located; however, the positions of the other portions of the two molecules could be very different.

For the ZOM, $H_{\text{NO}\bullet} = H_{\text{shell}}$, which is given by eq 3, except for Am12S. For Am12S, a small term $N(1-\alpha)V_{\text{water}}/V_{\text{shell}}$ where the volume of one water molecule $V_{\text{water}} = 30$ Å^3 must be added to eq 3 to account for the hydrogen bonding of the ammonium counterion.[13]

Departures from the ZOM. Figure 2 shows two schematic one-quarter cross sections of spherical micelles, drawn to scale with shell thickness $R_m - R_c = 5$ Å in both cases. In Figure 2a, $R_c = 16$ Å, growing to $R_c = 20$ Å in Figure 2b. This increase in R_c corresponds to approximately a doubling of the value of N for $N_c = 12$. Three zones are depicted through which NO• of probe types ZOM, I, and II diffuse, respectively. Each zone extends symmetrically about the center of the micelle; only portions are shown for clarity. The broken lines represent schematic diffusive paths. Zones I and II represent the simplest departures from the ZOM, maintaining the thickness of the polar shell, but displaced inward or outward. In Figure 2a, the inner surface of the NO• zone for probe I is displaced outward by a distance δ from the inner surface of the shell, and in Figure 2b, inward by δ. We use the convention that an outward displacement is positive, and an inward, negative. To simplify the language, we speak of a spin probe being "farther out" or "farther in" than the polar shell to mean $\delta > 0$ or $\delta < 0$, respectively. In this illustrative example, the zone for probe II maintains the same value of δ as the micelle grows.

Obviously, there are many possible departures from the ZOM, involving zones of greater or lesser thickness than the shell. In this paper, we restrict our attention to departures of the type shown in Figure 2 for simplicity because the additional parameters involved in more complicated zones are not yet justified by the information available.

We simplify the model by assuming that H_{shell} is uniform within the shell, $H = 0$ within the core, and $H = 1$ outside the shell. Furthermore, the diffusion motion of NO• samples all portions of the zone with equal probability, as illustrated in

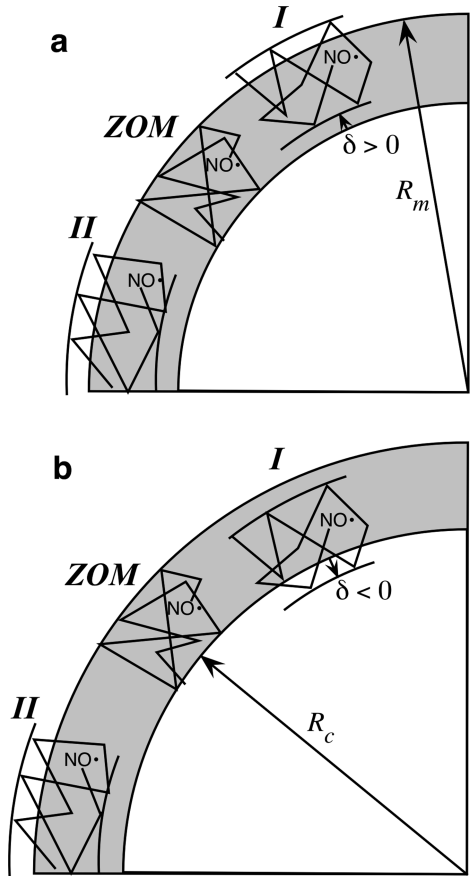

Figure 2. Diffusion zones of NO• for three types of nitroxide spin probes, I, II, and the zero-order model (ZOM). The thickness of the zones are equal to that of the shell. The zones extend concentrically around the micelle; only a portion is drawn for clarity. As the micelle grows from ***a*** to ***b*** by increasing the concentration of either the surfactant or added salt, I moves inward from residing outside the shell by $\delta > 0$ to inside by $\delta < 0$, while II maintains its position relative to the shell. The schematics are drawn to scale with shell thickness 5 Å for S12S with (a) $N = 60$ and (b) $N = 120$. The ZOM is the same as II with $\delta = 0$.

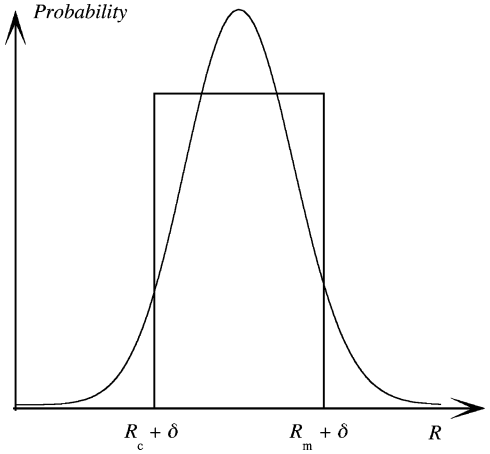

Figure 3. Schematic of the probability of finding NO• at a distance R from the center of the micelle, bell-shaped curve, and the constant-probability approximation, rectangle. For $\delta = 0$, the limits of the rectangle correspond to the polar shell; for $\delta < 0$ or $\delta > 0$, the limits are inside or outside the polar shell, respectively.

Figure 3. These assumptions could be relaxed at a cost of complexity that is not yet justified. For outward displacements of its zone, the average value of H sensed by NO• is easily shown to be the following:

$$H_{NO\bullet} = \frac{[R_m{}^3 - (R_c + \delta)^3]H_{shell} + \delta^3}{(R_m + \delta)^3 - (R_c + \delta)^3}; \qquad 0 < \delta < t_s \quad (9)$$

where the shell thickness $t_s = R_m - R_c$. The term δ^3 in the numerator results from inserting the value of $H = 1$ for water. For inward displacements,

$$H_{NO\bullet} = \frac{[(R_m + \delta)^3 - R_c{}^3]H_{shell}}{(R_m + \delta)^3 - (R_c + \delta)^3}; \qquad 0 > \delta > -t_s \quad (10)$$

For the ZOM, $\delta = 0$ and both eq 9 and 10 reduce to H_{shell}. Outside of the limits on δ in eqs 9 and 10, $H_{NO\bullet} = 1$ or 0, respectively.

In the example of Figure 2, the average value of $H_{NO\bullet}$ of probe I would decrease more rapidly than H_{shell} as the micelle grows, while that of probe II would decrease at nearly the same rate as H_{shell}. The probability of collision of NO• in zone I with a spectroscopic probe in zone II would decrease as the micelle grows because the overlap region of their respective zones decreases. The spectroscopic probe in zone II could be another NO• or, perhaps, pyrene (or some other fluorophore). We mention this because the rate of collision between a benchmark probe and another is an additional way to fix their relative positions in the micelle. Similarly, the probability of collision of NO• in zone I with a ZOM probe would first increase and then decrease during the progression from Figure 2a to b.

Materials and Methods

This work is a continuation of a recently published paper[18] in which most of the materials, their treatment, sample preparation, EPR experiments, and data analysis were detailed. All measurements were at 25 °C except for a few measurements of 16DSE in Am12S at 16 and 35 °C. Briefly, approximately 500 mM micelle solutions without added NaCl were prepared with a spin probe/surfactant molar ratio of 1:500. These mother solutions were diluted with distilled water with or without added NaCl to produce zero-salt or add-salt samples while maintaining the same spin probe/surfactant molar ratio. Approximately conjugate pairs of add-salt and zero-salt samples were prepared, i.e., pairs of samples with approximately the same value of N.[18] A brief experiment using hexadecyltrimethylammonium chloride was conducted as described below.

Results

Figure 4a, prepared mostly from data in the literature, shows values of $H_{NO\bullet}$ as functions of N for 5DSE (circles)[17] and 16DSE (diamonds),[23] respectively, in S12S micelles. In Figures 4−6 and 8, closed or open symbols represent data from add-salt or zero-salt samples, respectively. To obtain another zero-salt point near $N = 130$, which is near the sphere−rod transition,[7] a 1.01 M S12S sample was measured with 5DSE. The line through the 5DSE data is derived from the ZOM, i.e., $H_{NO\bullet} = H_{shell}$ derived from eqs 3−7 by using one adjustable parameter, yielding values of V_{hg} and N_{wet} given in Table 1. Figure 4a reiterates the fact that 5DSE is in accord with the ZOM in S12S; however, clearly, 16DSE is not. At low values of N, 16DSE is farther out than 5DSE and at larger values of N, farther in. As a reminder that one cannot be too cautious, we note that, near $N = 68$, the two probes report the same value of $H_{NO\bullet}$, i.e., they occupy the same position in the micelle. Often, 0.1 M surfactant has been employed in many micelle investigations, including those of Kevan and co-workers,[3,4] where, for S12S, coincidentally, $N = 68$. Thus, conclusions drawn at one

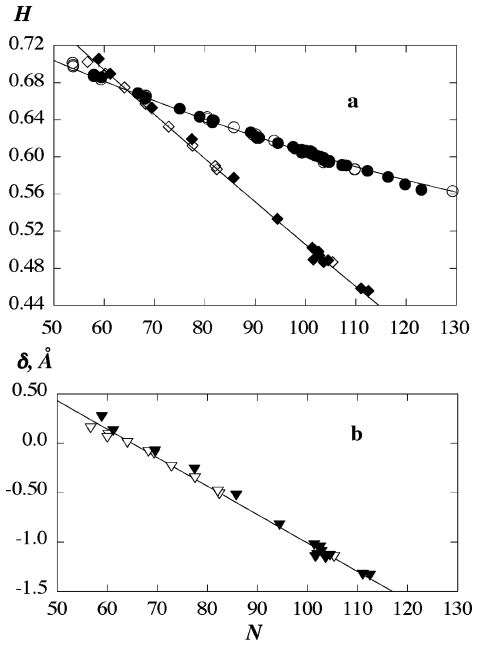

Figure 4. (a) Volume fraction of water in the zones occupied by 5DSE (○, ●) and 16DSE (◇, ◆) vs the aggregation number of S12S, 25 °C; data from the literature 5DSE[17] and 16DSE[23] except for the one point near $N = 130$ measured with 5DSE in [S12S] = 1.01 M without added salt. Filled and open symbols correspond to add-salt and zero-salt samples, respectively. Clusters of points near $N = 100$ for both spin probes are from approximately constant C_{aq} series. The solid line through the 5DSE data is the ZOM, eqs 3−7, with vertical position fixed by one parameter, either N_{wet} or V_{hg}, listed in Table 1; the slope is not adjustable. The line through the 16DSE data is eq 9 or 10 using δ given by the solid line in (b). (b) 16DSE diffusion zone displacement (▽, ▼) computed from eq 9 or 10 vs the aggregation number. The solid line is a linear least-squares fit $\delta = 0.45 \pm 0.02 - 0.029(N - N^0)$ with coefficient of correlation, $r = 0.997$.

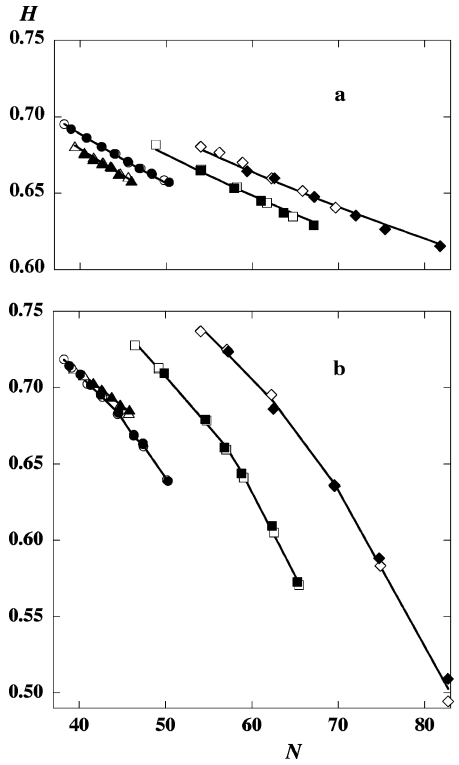

Figure 5. (a) Volume fraction of water in the zones occupied by 5DSE vs the aggregation number of S8S (△, ▲), S9S (○, ●), S10S (□, ■), and S11S (◇, ◆) micelles, 25 °C. The solid lines are computed from the ZOM, eqs 3−7, with vertical positions fixed by one parameter, either N_{wet} or V_{hg} listed in Table 1; the slopes are not adjustable. (b) Volume fraction of water in the zones occupied by 16DSE; same symbols as in (a). The lines through the 16DSE data are to guide the eye. Filled and open symbols correspond to add-salt and zero-salt samples, respectively.

surfactant concentration cannot safely be extrapolated to other concentrations or to samples with added salt. We cannot resist admitting that one of us fell exactly into this trap in the early days of this work, measuring A_+ for a series of *x*DSE in 0.1 SDS, finding them to be nearly equal, and being misled for some time into the working hypothesis that all were in the same position at other surfactant concentrations or with added salt.

For each 16DSE datum in Figure 4a, a value of δ was determined to satisfy either eq 9 or 10, depending on whether δ was positive or negative. These calculations were carried out by trial and error in a spreadsheet, adjusting δ until the computed and measured value of H_{NO}• matched. The resulting values of δ are plotted in Figure 4b, showing that they turn out to vary linearly with *N*. The solid line is a linear least-squares fit yielding $\delta = 0.45 \pm 0.02 - 0.029\ (N - N^0)$ with coefficient of correlation, $r = 0.997$. N^0 appropriate for S12S is given in Table 1. Thus, employing the model of molecule I of Figure 2, NO• in 16DSE moves from being displaced 0.45 Å outside the polar shell at $N^0 = 50$, (at the cmc_0) to approximately 1.3 Å inside. Thus, even though the difference in the two spin probes appears to be dramatic in Figure 4a, they both largely occupy the polar shell; 5DSE entirely and 16DSE with 85% probability averaged from $N = 60$ to 113. The excellent precision attainable in measurement of A_+ permits rather precise values of δ to be obtained. The precision available from such measurements and precautions required to obtain such precision have been discussed.[17]

Values of H_{NO}• are available in the literature[13] for 5DSE in Am12S, where the ZOM was found to apply. See Table 1. In this work, we have measured 16DSE in this surfactant, and a plot of H_{NO}• as a function of *N* at 25 °C (not shown) for Am12S is very similar to Figure 4a. The lines for 5DSE and 16DSE cross at about $N = 87$. We have very limited data at 16 and 35 °C; however, they are quite interesting, so we decided to include them.

Figure 5a shows values of H_{NO}• for 5DSE and Figure 5b for 16DSE as functions of *N* in SN_cS micelles, $N_c = 8-11$. The lines through the 5DSE data are all derived from the ZOM with one adjustable parameter given in Table 1. Note that the scale of the ordinate is the same in Figure 5a and b, only the origin is different. Clearly, the ZOM describes the behavior of 5DSE well and not 16DSE, as is evident from the fact the curves for the two probes are significantly different. Figures 4 and 5 are representative of data in all SN_cS micelles, indeed, in all micelles studied to date in that the values of H_{NO}• are similar for the two probes. Nevertheless, there are differences that are easily discernible. Therefore, within the precision afforded by the EPR spin-probe method, it is clear that 16DSE cannot be described by the ZOM.

The 16DSE data in SN_cS micelles were interpreted in the same way as in S12S, the results of the departures from the ZOM being displayed in Figure 6a. For all SN_cS micelles except S8S, the zone of diffusion of NO• for 16DSE varies from extending slightly outside the shell to slightly inside as the micelles grow due to increasing either surfactant or salt concentrations. Unlike S12S and Am12S, where δ varies linearly with *N*, there appears to be a slight curvature to the lines in Figure 6a, except for S8S. Note that the schematic departure depicted for I in Figure 2 gives a visual idea of the departures,

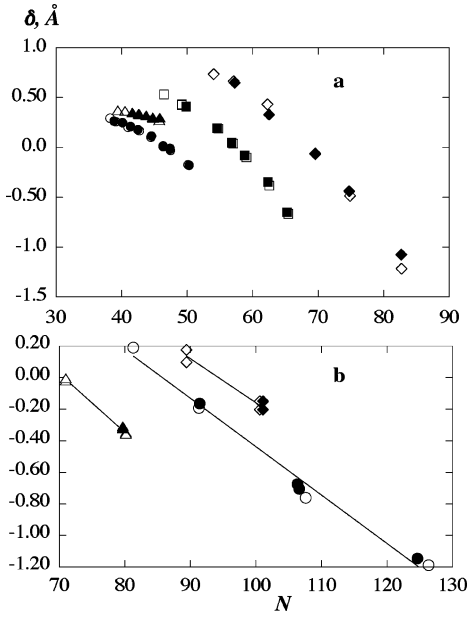

Figure 6. (a) Shift of diffusion zone of 16DSE with the aggregation number for S8S−S11S(x) micelles; same symbols as Figure 5. (b) Zone displacements for Am12S at 16° (◇, ◆), 25° (○, ●), and 35°C (△, ▲). Filled and open symbols correspond to add-salt and zero-salt samples, respectively. For $\delta = 0$, the diffusion zone of 16DSE coincides with the shell; these occur near similar values of H_{shell} of each surfactant. These displacements are comparable with those depicted for I in Figure 1.

being drawn to be from $\delta = +1$ Å in Figure 2a to -1 Å in Figure 2b, comparable to the experimental values in Figures 4a and 6.

Figure 6b shows departures of 16DSE from the ZOM in AmDS at three temperatures. At 25 °C, the ZOM is represented by the dashed curve in Figure 5 of ref 13. By using that curve as H_{shell}, values of δ were derived from 16DSE data from eq 9 or 10. At 16 and 35 °C, 5DSE data taken in ref 13 were analyzed under the additional assumption that 5DSE does not depart from the ZOM when the temperature is changed modestly. Until this, albeit reasonable, assumption is checked further, the values of δ given in Figure 6b for 16 and 35°C must be considered to be tentative. Note that a slight drying of the polar shell of Am12S occurs under this assumption as the temperature is raised from 16 to 35 °C, where V_{hg} increases from 127 to 129 Å^3 with $N_{wet} = 0$, or alternatively, N_{wet} increases from 1.88 to 2.20 with $V_{hg} = 66.4$ Å^3 over this temperature range. See Table 1. The present measurements of 16DSE were then used to obtain values of δ given in Figure 6b.

It is premature to propose a detailed model that predicts the position of NO• for 16DSE as a function of various micelle parameters, including temperature. Spin probes xDSE, $x = 6$, 7, 10, 12, and 17 are also available for study; a good model would have to predict the location of NO• for all of those. Nevertheless, we can gain valuable insight from the limited data that we have. For example, when we began the study, we thought that the fact that 16DSE had two hydrophilic groups widely separated, both of which presumably would adhere approximately to the ZOM, would mean that the size of the core would dominate the position of NO•. This would mean that plots of δ versus R_c would be similar for all SN_cS and for Am12D. However, a plot of δ versus R_c, (not shown) looks very much like Figure 6a. Therefore, it is clear that δ does not correlate with R_c. We did notice that, at $\delta = 0$, where 16DSE occupies the shell, H_{shell} is similar for all of the surfactants.

Thus, we prepared Figure 7, showing the displacements of

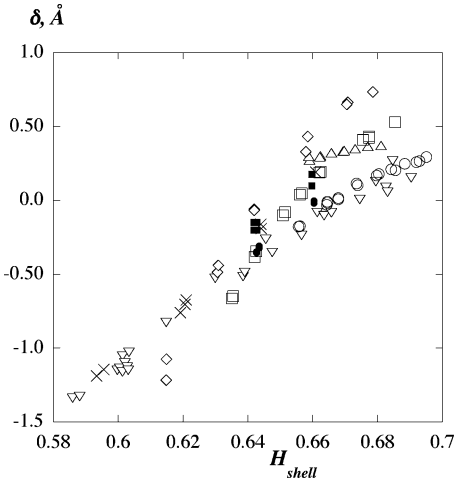

Figure 7. 16DSE zone displacements vs the volume fraction of water in the polar shell for SN_cS micelles, $N_c = 8$ (△), 9 (○), 10 (□), 11 (◇), and 12 (▽), 25 °C; Am12S at 25°C (×), 16°C (■), and 35°C (●). For clarity, the add-salt and zero-salt data are not distinguished. For $\delta = 0$, the diffusion zone of 16DSE coincides with the shell; these occur near similar values of $H_{shell} = 0.66$ for all of the surfactants and for Am12S at three temperatures.

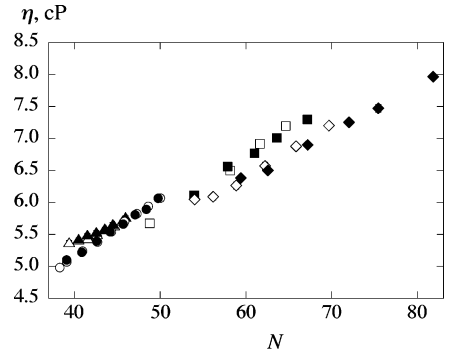

Figure 8. Microviscosity of SN_cS micelles vs aggregation number, 25 °C. Same symbols as in Figure 5.

NO• for 16DSE in all of the surfactants at 25 °C and in Am12S at 16 and 35 °C as a function of H_{shell}. Figure 7 is too complicated as it is, thus we have not distinguished between zero-salt and add-salt data. Despite some scatter, it is clear the displacements are correlated with H_{shell}. For all the surfactants, δ is zero near $H_{shell} = 0.66$, that is to say that NO• for 16DSE moves inward if the shell is less polar and outward if it is more polar. Particularly interesting is the fact that the limited data for Am12S at 16 and 35 °C also seem to be correlated with H_{shell} those data (solid circles and squares) falling near the common line in Figure 7. If this holds up under further investigation, then this means that movement NO• of 16DSE as a function of temperature is not governed by geometry (e.g., R_c), rather by the amount of water in the shell. We now cautiously speculate that the reason 5DSE adheres to the ZOM is because it has two hydrophilic groups in close proximity that serve to limit diffusion of NO• to within the polar shell. This hypothesis may be tested in the future by using a doxylalkane instead of the acid ester.

Microviscosity of the Polar Shell. The same spectra collected for the main purpose of the paper also yield estimates of the microviscosity of the polar shell, thus, we present those data in Figure 8 for $N_c = 8-11$. See, for example, ref 12 for a detailed account of how microviscosities of micelles are deduced from the rotational correlation times of NO•, taking into account the rotation of the micelles as a whole. These times were obtained

from the line height ratios,[39] and microviscosities were computed as recently detailed.[21] The variation of the microviscosity with N is modest and seems to be similar at the same value of N for all values of N_c. Comparing Figure 8 with Figure 9 of ref 21 shows that the microviscosity in these micelles and its variation with N are very similar to those in S12S, dodecyl trimethlyammonium chloride (DTAC), and DTAB. In every case, the microviscosity depends only on N in zero-salt or add-salt samples. This means that the microviscosity does not depend on the concentration of micelles, i.e., it does not depend on intermicelle interactions.

Discussion

All of the solid lines through the 5DSE data in Figures 4a and 5a as well as Figure 5 of ref 13 result from fixing $V_{hg} = 129 \pm 1$ Å^3 (average and standard deviation in Table 1) assuming $N_{wet} = 0$ or, alternatively, $N_{wet} = 1.90 \pm 0.1$ assuming $V_{hg} = 66.4$ Å^3. These are reasonable values: N_{wet} is approximately equal to 2 is often quoted[40,41] to be the number of methylene groups exposed to water. The number of water molecules in the shell per headgroup, N_{water}, is easily calculated; for S12S, this results in about $N_{water} = 9$ at $N = 63$, in satisfactory agreement with estimates from transport properties.[15] By using space-filling models, Szajdzinska-Pietek et al.[4] estimated $N_{water} = 9$ in 0.1 M S12S. Further comparison of the absolute values of eq 1 compared with estimates from other techniques may be found in recent papers;[7,12] however, our argument that 5DSE is described by the ZOM is not based on the absolute values, rather that they are describe by the same hydration model in all SN_cS and Am12S versus variations in both N and N_c. Any movement of NO$^\bullet$ with either N or N_c larger than approximately 0.2 Å would be easily detected as the results with 16DSE demonstrate.

The possibility exists that the shell thickness and the position of 5DSE could both change in exactly the right way as to compensate one another and give the illusion of the ZOM, but this is quite unlikely. The variation of $H_{NO^\bullet}$ with N for any given surfactant could be rationalized in terms of either the strict ZOM or a type II model with small, constant δ (Figure 2). The fact that the adjustable parameter V_{hg} (or N_{wet}) is the same for all N_c argues against this interpretation because the same constant value of δ would have to be maintained as the relative dimensions of the surfactant and probe varied; again, unlikely.

Turning to the displacements of 16DSE, we see that, as fractions of the shell thickness, the maximum departures from the ZOM vary from a minimum of 6% for S9S to 23% for S11S, with an average maximum departure in all surfactants of 14%. These departures are similar to an average departure of 16% needed to rationalize the quenching of pyrene by dodecylpyridinium chloride in a series of tetraalkylammonium dodecyl sulfate micelles employing a simple hydrodynamic model of bimolecular collisions.[25] In the previous work, we were only able to find the relative departures of pyrene with respect to dodecylpyridinium chloride, having, at that time, no way to locate either with respect to the micelle.

To our knowledge, the only work that attempted to define the position of doxylstearate in dodecyl sulfate micelles is that of Kevan and co-workers who worked with frozen solutions measuring the modulation of electron spin−echoes (ESEM) by deuterium.[3,4] Those elegant experiments employed spin probes similar to those in Scheme 1, except they were the acids (xDSA), not the esters, labeled at $x = 5$, 7, 10, 12, and 16. By selectively deuterating moieties of the surfactants or by using D_2O rather than water as the solvent, those authors proposed a scheme in

SCHEME 1

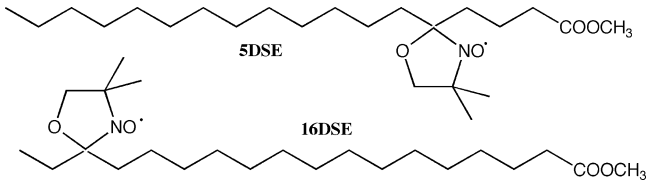

which all of the probes assumed the same conformation and the variation in the position of NO$^\bullet$ resulted from bending of the alkyl chains. Those authors assumed that the carboxyl groups were anchored in the shell, beginning with a radial intrusion into the core. They concluded that NO$^\bullet$ for the series of spin probes resided near the surface as we have concluded for 5DSE and 16DSE. However, their proposed detailed positions as being at various depths within the core are at odds with our results. In terms of our definition of δ, values of δ up to −6 Å were proposed, which would result in $H_{NO^\bullet}$ near zero. The interpretation of ESEM experiments is difficult, because the modulation depths are complicated functions of both the number of interacting deuterons and their distances from NO$^\bullet$.[3,4] It would be very interesting, after our work is complete employing other xDSE probes, to see if the ESEM results could be successfully interpreted within the same model that we employ. For example, could the positions of NO$^\bullet$ be fixed at our values and a reasonable number of interacting deuterons be deduced?

In more recent work, Szajdzinska-Pietek and co-workers[5] measured the first-order rate constant of quenching of pyrene, k_q, by xDSE ($x = 5$, 10, and 12) in hexadecyltrimethylammonium chloride (CTAC) micelles. Her and her co-worker's results are shown in Figure 9, showing that k_q is about the same for $x = 5$ and 10 and slightly smaller for $x = 12$. They[5] interpreted the differences in the values of k_q in terms of different pyrene−quencher pair distances. By using the ESE data described in the previous paragraph as a basis for locating NO$^\bullet$ (in the core), they suggested that pyrene was near the surface and that 12DSE was buried slightly deeper than 5- and 10DSE into the core. Time-resolved fluorescence quenching by spin probes is particularly interesting because, unlike most of the other standard quenchers, high precision information is available from EPR by using those same quenchers.

Unfortunately, EPR measurements were not reported,[5] so we carried out a brief experiment in 0.1 M CTAC (Fluka, as received) at 25 °C, employing 5-, 10-, and 12DSE obtained from Molecular Probes. The calibrations of A_+ versus $H_{NO^\bullet}$ were not available for 10 or 12DSE, thus these were carried out as detailed in the Appendix. Anticipating that 6- and 7DSE will be useful probes, they were also included in the calibrations.

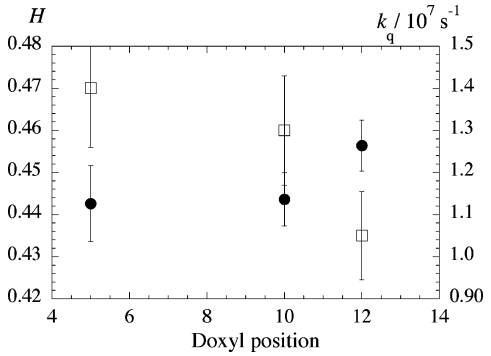

Figure 9. Volume fraction of water in the zones occupied by 5, 10, and 12DSE (●, left-hand coordinate) and the rate constant of quenching of pyrene (□, right-hand coordinate)[5] by these same spin probes vs label position in 0.1 M CTAC micelles, 25 °C.

Furthermore, the same spectra may be employed to estimate the values of the hydrodynamic radii needed to measure microviscosities,[42] so these were determined as well. The results are gathered into Table 2 for future reference.

In CTAC micelles, typical well-resolved three-line EPR spectra were observed.[24] Values of H_{NO}• were computed from eq 8 from measured values of A_+, using the parameters in Table 2 and are displayed in Figure 9. H_{NO}• is about the same for $x = 5$ and 10 and slightly larger for $x = 12$. Thus, values of both H_{NO}• and k_q are the same within experimental uncertainty for $x = 5$ and 10 and marginally different for $x = 12$. From H_{NO}• we learn that NO• for each of these spin probes is positioned similarly relative to the micelle and from k_q similarly with respect to pyrene. For $x = 12$, H_{NO}• indicates that NO• is slightly farther out than $x = 5$ and 10 (higher value of H_{NO}•), opposite to the proposal in ref 5, while k_q shows that NO• is slightly farther from pyrene (lower value of k_q). Taken together, the $x = 12$ results, to the extent that they are significantly different from $x = 5$ and 10, show that pyrene is farther into the micelle than NO•.

Quantitative positions of NO• (values of δ) must await more work to determine the parameters needed to calculate H_{shell} and, importantly, to investigate values of δ as functions of N; however, it is already clear that NO• cannot be located in the core where $H = 0$. It remains to be demonstrated that 5DSE follows the ZOM in CTAC micelles, however, it likely does because it does so in the shorter chain surfactant DTAB, as shown in the companion paper.[16] As Figure 4a reminds us, Figure 9 could be quite different at other surfactant concentrations or in the presence of added salt.

Values of k_q in micelles may be successfully modeled by the Stokes−Einstein−Smoluchowski equation, as has been shown in recent papers.[10,12] All of the information needed is available from EPR and TRFQ. The extent of overlap of the zones occupied by pyrene and NO• governs the observed probability of quenching and thus leads directly to an estimate of the distance between the fluorophore and quencher. See, for example, eqs 12 and 13 of ref 10. Thus, EPR and TRFQ taken together have the potential to locate both pyrene and NO•, labeled in various positions, after a full investigation.

Conclusions

The agreement between the variation of H_{NO}• and H_{shell} for 5DSE as a function of N in any one of the SN_cS micelles shows that either the ZOM or a zone of type II in Figure 2 describes the zone through which this spin probe diffuses. Because the values of the one adjustable parameter are reasonable, δ for zone II would be rather small. The agreement between the variation of H_{NO}• and H_{shell} for 5DSE as a function of N_c in all of the SN_cS micelles and Am12S shows that either the same value of δ for a type II zone is obtained for all the micelles or that the ZOM is obtained. Because the former is unlikely, we propose the latter, making 5DSE a good benchmark probe. A nitroxide spin probe is particularly suited to be a benchmark because the location of NO•, confined to the unpaired spin−orbital, is well defined. As a negation of the hypothesis that 5DSE follows the ZOM, we show that 16DSE does not. Small displacements of NO• as functions of N and N_c bring theory and experiment into agreement. These displacements are well correlated with the volume fraction of the polar shell occupied by water. Departures from the ZOM as small as 0.2 Å may be detected.

Appendix. Calibration of *x*DSE Spin Probes

Methods to calibrate spin probes have been described in detail as follows: H_{NO}• versus A_+ for 16DSE[11] and 5DSE[13] and the hydrodynamic radii for 16DSE[12] and 5DSE.[42] Those references may be consulted for details about the procedures, theory, background, and error estimates. Briefly, the spin probes are dissolved into water−methanol mixtures at a low concentration. Parameters for eq 8 are obtained by fitting the measured values of A_+ to the values of H_{NO}• computed from eq A1 of ref 13. The same spectra contain information needed to obtain the hydrodynamic radii, R_h, from the Debye−Stokes−Einstein equation[43]

$$\tau = \frac{4\pi\eta R_h^3}{3kT} \tag{A1}$$

where τ is the rotational correlation time of NO•, η is the shear viscosity of the solvent, k the Boltzmann constant, and T the absolute temperature. The application of eq A1 to spin probes was discussed in great detail in ref 42 and references therein. The value of R_h in eq A1 for flexible molecules often does not correspond accurately to the geometrical value for the entire molecule computed from van der Waals radii, for example, by the method of Bondi;[44] however, if R_h is constant as the solvent, temperature, and viscosity are changed, then eq A1 may be used to measure viscosity.

Probes *x*DSE, $x = 6$, 7, 10, and 12 were purchased from Molecular Probes (Eugene, OR) and used as received. A spin probe concentration of 5×10^{-5} M was routinely used; however, a few measurements were taken at one-half this concentration to confirm that spin exchange-induced line shifts[45] were negligible. Values of A_+ were measured from five spectra taken one after another, averaged, and plotted versus H_{NO}•. These plots were linear in every case; see, for example, Figure 7 of ref. 13. These data were fit to eq 8, yielding the data in Table 2. Previous calibrations of 5DSE[13] and 16DSE[12] are included in Table 2 for convenience. Values of τ computed from line height ratios,[46] corrected for inhomogeneous line broadening,[47] were fit to eq A1 by employing the known viscosities of the solvent mixtures.[48] For each *x*DSE, the values of R_h were constant as a function of η, i.e., plots of τ were linear in η/T.[12] It has been known for some time that values of R_h for flexible spin probes such as *x*DSE are a function of the label position,[12] and Table 2 bears that out. Nevertheless, except for 16DSE, they do not show a dramatic variation, modestly declining from a maximum for label positions near the center of the stearic acid chain to smaller values near the ends.

Acknowledgment. We gratefully acknowledge support from NIH/MBRS S06 GM48680-09 and RFFI (04-03-32604-a and 05-04-48632-a).

References and Notes

(1) Grieser, F.; Drummond, C. J. *J. Phys. Chem.* **1988**, *92*, 5580.
(2) Almgren, M.; Grieser, F.; Thomas, J. K. *J. Am. Chem. Soc.* **1979**, *101*, 279.
(3) Szajdzinska-Pietek, E.; Maldonado, R.; Kevan, L.; Berr, S. S.; Jones, R. R. M. *J. Phys. Chem.* **1985**, *89*, 1547.
(4) Szajdzinska-Pietek, E.; Maldonado, R.; Kevan, L.; Jones, R. R. M.; Coleman, M. J. *J. Am. Chem. Soc.* **1985**, *107*, 784.
(5) Szajdzinska-Pietek, E.; Wolszak, M. *Chem. Phys. Lett.* **1997**, *270*, 527.
(6) Szajdzinska-Pietek, E.; Gebicki, J. L. *J. Phys. Chem.* **1995**, *99*, 13500.
(7) Bales, B. L.; Messina, L.; Vidal, A.; Peric, M.; Nascimento, O. R. *J. Phys. Chem. B* **1998**, *102*, 10347.

(8) Bales, B. L.; Shahin, A.; Lindblad, C.; Almgren, M. *J. Phys. Chem. B* **2000**, *104*, 256.
(9) Ranganathan, R.; Peric, M.; Medina, R.; Garcia, U.; Bales, B. L.; Almgren, M. *Langmuir* **2001**, *17*, 6765.
(10) Ranganathan, R.; Vautier-Giongo, C.; Bales, B. L. *J. Phys. Chem. B* **2003**, *107*, 10312.
(11) Bales, B. L.; Howe, A. M.; Pitt, A. R.; Roe, J. A.; Griffiths, P. C. *J. Phys. Chem. B* **2000**, *104*, 264.
(12) Bales, B. L.; Ranaganathan, R.; Griffiths, P. C. *J. Phys. Chem. B* **2001**, *105*, 7465.
(13) Tcacenco, C. M.; Zana, R.; Bales, B. L. *J. Phys. Chem. B* **2005**, *109*, 15997.
(14) Lindman, B.; Wennerström, H.; Gustavsson, H.; Kamenka, N.; Brun, B. *Pure Appl. Chem.* **1980**, *52*, 1307.
(15) Tokiwa, F.; Ohki, K. *J. Phys. Chem.* **1967**, *71*, 1343.
(16) Lebedeva, N. V.; Bales, B. L. *J. Phys. Chem. B* **2006**, *110*, 9800.
(17) Bales, B. L. *J. Phys. Chem. B* **2001**, *105*, 6798.
(18) Lebedeva, N. V.; Shahine, A.; Bales, B. L. *J. Phys. Chem. B* **2005**, *109*, 19806.
(19) Anacker, E. W.; Rush, R. M.; Johnson, J. S. *J. Phys. Chem.* **1964**, *68*, 81.
(20) Huisman, H. F. *Proc. K. Ned. Akad. Wet., Ser. B: Phys. Sci.* **1964**, *67*, 367.
(21) Bales, B. L.; Zana, R. *J. Phys. Chem. B* **2002**, *106*, 1926.
(22) Quina, F. H.; Nassar, P. M.; Bonilha, J. B. S.; Bales, B. L. *J. Phys. Chem.* **1995**, *99*, 17028.
(23) Bales, B. L. An Aggregation Number-Based Definition of the Ionization of a Micelle. Demonstration with TRFQ, SANS, and EPR. In *Magnetic Resonance in Colloid and Interface Science*; Fraissard, J., Lapina, O., Eds.; Kluwer Academic Publishers: Dordrecht, 2002; Vol. 76; p 277.
(24) Bales, B. L.; Tiguida, K.; Zana, R. *J. Phys. Chem. B* **2004**, *108*, 14948.
(25) Bales, B. L.; Benrraou, M.; Tiguida, K.; Zana, R. *J. Phys. Chem. B* **2005**, *109*, 7987.
(26) MacKerell A. D., Jr. *J. Phys. Chem.* **1995**, *99*, 1846
(27) http://www.csun.edu/supramolecularstudies/micelle.html.
(28) Tanford, C. *The Hydrophobic Effect: Formation of Micelles and Biological Membranes.*, 2nd ed.; Wiley-Interscience: New York, 1980.
(29) Cabane, B. Small-Angle Scattering Methods. In *Surfactant Solutions: New Methods of Investigation*; Zana, R., Ed.; Marcel Dekker: New York, 1987; Vol. 22; p 57.
(30) Ramachandran, C.; Pyter, R. A.; Mukerjee, P. *J. Phys. Chem.* **1982**, *86*, 3198.
(31) Mukerjee, P.; Ramachandran, C.; Pyter, R. A. *J. Phys. Chem.* **1982**, *86*, 3189.
(32) Pyter, R. A.; Ramachandran, C.; Mukerjee, P. *J. Phys. Chem.* **1982**, *86*, 3206.
(33) Schwartz, R. N.; Peric, M.; Smith, S. A.; Bales, B. L. *J. Phys. Chem. B* **1997**, *101*, 8735.
(34) Griffith, O. H.; Dehlinger, P. J.; Van, S. P. *J. Membr. Biol.* **1974**, *15*, 159.
(35) Knauer, B. R.; Napier, J. J. *J. Am. Chem. Soc.* **1976**, *98*, 4395.
(36) Reddock, A. H.; Konishi, S. *J. Chem. Phys.* **1979**, *70*, 2121.
(37) Abe, T.; Tero-Kubota, S.; Ikegami, Y. *J. Phys. Chem.* **1982**, *86*, 1358.
(38) Jackson, S. E.; Smith, E. A.; Symons, M. C. R. *Discuss. Faraday Soc.* **1978**, *64*, 173.
(39) Schreier, S.; Polnaszek, C. F.; Smith, I. C. P. *Biochim. Biophys. Acta* **1978**, *515*, 375.
(40) Halle, B.; Carlström, G. *J. Phys. Chem.* **1981**, *85*, 2142.
(41) Triolo, R.; Caponetti, E.; Graziano, V. *J. Phys. Chem.* **1985**, *89*, 5743.
(42) Bales, B. L.; Stenland, C. *J. Phys. Chem.* **1993**, *97*, 3418.
(43) Jones, L. L.; Schwartz, R. N. *Mol. Phys.* **1981**, *43*, 527.
(44) Bondi, A. *J. Phys. Chem.* **1964**, *68*, 441.
(45) Bales, B. L.; Peric, M. *J. Phys. Chem. B* **1997**, *101*, 8707.
(46) Marsh, D. Experimental Methods in Spin-Label Spectral Analysis. In *Spin Labeling. Theory and Applications*; Plenum Publishing Corporation: New York, 1989; Vol. 8; p 255.
(47) Bales, B. L. Inhomogeneously Broadened Spin-Label Spectra. In *Biological Magnetic Resonance*; L. J. Berliner, L. J., Reuben, J., Eds.; Plenum Publishing Corporation: New York, 1989; Vol. 8; p 77.
(48) Vargaftik, N. B. *Tables on the Thermophysical Properties of Liquids and Gases*, 2nd ed.; Hemisphere Publishing: Washington, DC, 1975; Vol. IV (English translation).
(49) Bales, B. L.; Almgren, M. *J. Phys. Chem.* **1995**, *99*, 15153.
(50) Ranganathan, R.; Peric, M.; Bales, B. L. *J. Phys. Chem. B* **1998**, *102*, 8436.